Constraining the location of the emitting region in *Fermi* blazars through rapid gamma–ray variability

F. Tavecchio[★], G. Ghisellini, G. Bonnoli, G. Ghirlanda
INAF – Osservatorio Astronomico di Brera, via E. Bianchi 46, I–23807 Merate, Italy

12 April 2010

ABSTRACT

We consider the 1.5 years *Fermi*/Large Area Telescope light curves ($E > 100$ MeV) of the flat spectrum radio quasars 3C 454.3 and PKS 1510–089, which show high activity in this period of time. We characterise the *duty cycle* of the source by comparing the time spent by the sources at different flux levels. We consider in detail the light curves covering periods of extreme flux. The large number of high–energy photons collected by LAT in these events allows us to find evidence of variability on timescales of *few hours*. We discuss the implications of significant variability on such short timescales, that challenge the scenario recently advanced in which the bulk of the γ–ray luminosity is produced in regions of the jet at large distances (tens of parsec) from the black hole.

Key words: galaxies: jets – galaxies: individual: 3C 454.3 - PKS 1510–089 – radiation mechanisms: non–thermal – gamma-rays: observations.

1 INTRODUCTION

Powerful γ–ray emission is a distinctive feature of Flat Spectrum Radio Quasars (FSRQs), radio–loud active galactic nuclei with the relativistic jet closely oriented towards the Earth. Gamma rays with energy above 100 MeV from these sources are widely believed to be produced through the inverse Compton (IC) scattering between highly relativistic electrons in the jet and ambient photons, either the optical–UV photons from the accretion disk (e.g. Dermer & Schlickeiser 1993) or reprocessed by the gas in the broad line region (BLR, e.g. Sikora et al. 1994) or the infra–red photons from the dusty torus (e.g. Blazejowski et al. 2000).

The sources of target photons dominating the IC emission is basically determined by the location of the emitting region in the jet (e.g. Ghisellini & Tavecchio 2009, Sikora et al. 2009). Nuclear optical–UV seed photons dominate if γ–rays are produced inside the BLR (at distances <0.1–1 pc). On the contrary, if the emission occurs at larger distances, the dominating population of target photons will be that from the torus. In turn, the location of the γ–ray production and nature of the target photons determines some of the quantities derived from the radiative models, such as electron energies and cooling times, jet power, magnetic field intensity.

The overall spectral energy distributions of FSRQs can be well reproduced assuming an emission region located at 300–1000 Schwarzschild radii from the central black hole (e.g. Ghisellini et al. 2010). However, recently, several authors (Sikora et al. 2008; Larionov et al. 2008; Marscher et al. 2008, 2010) argued that the bulk of the emission, especially during large outbursts, is produced at larger distances, even at distances of the order of 10–20 pc from

the central black hole, at the expected location of a reconfinement shock (e.g. Sokolov et al. 2004). The main arguments advanced to support this conclusion come from observations in the radio band coupled with the observed peculiar behaviour of the polarisation angle in the optical. This led Marscher et al. (2008) to suggest a general scenario in which blobs (or knots) of material ejected from the central region are forced by the magnetic field to follow an helical path, accounting for the observed rotation of the polarisation angle in the optical. These knots are opaque in the radio band until they reach large distances. The transition to transparency is marked in VLBI maps by the passage of the compact radio core, after which knots become visible and their trajectories can be directly traced. The passage of the knots from the core, interpreted as the location of a standing conical shock, is marked by the huge flares at all wavelengths, triggered by the compression of the plasma in the shock. This scenario has important consequences for the variability of the emission: since the emission region is located at large distances from the central engine, their size is probably large, even if a very small jet opening angle ($\theta_{\rm jet} < 1$ deg) is assumed. Quantitatively, the light crossing time of the source put a lower limit on the variability timescale expressed as: $t_{\rm var} > \theta_{\rm jet}d(1+z)/c\delta$, where d is the distance of the emission region from the central engine and δ the relativistic Doppler factor. Assuming $d = 15$ pc, $\theta_{\rm jet} = 0.1$ deg and $\delta = 20$ we find $t_{\rm var} > 1.5(1 + z)$ days. Therefore, variability at timescales below 1 day, especially at γ–ray energies, would be rather difficult to accommodate in this scheme.

The Large Area Telescope (LAT) onboard *Fermi* (Atwood at al. 2009), with its continuous monitoring of the sky, is the ideal instrument to investigate the possible existence of rapid (timescale $t_{\rm var} < 1$ day) γ–ray variability in FSRQs. Indeed, variability on timescale of 12 hours has been already reported for the FSRQs
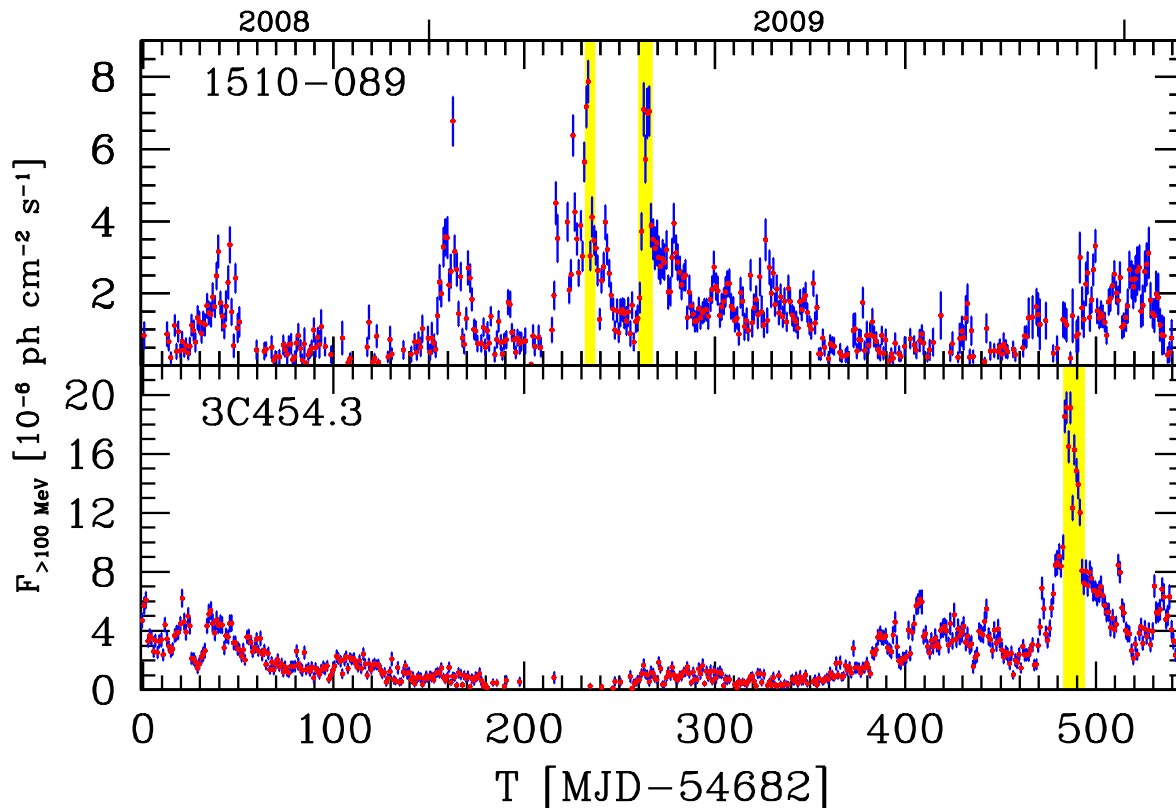
★ E–mail: fabrizio.tavecchio@brera.inaf.it

Figure 1. Light curve of PKS 1510–089 (upper panel) and 3C 454.3 (lower panel) from 2008 August 4 (MJD 54682) to 2010 January 31 (MJD 55228) in bins of 1 day. Vertical yellow stripes show the periods of large flux studied in detail in this work.

PKS 1454–354 ($z = 1.424$; Abdo et al. 2009) and PKS 1502+105 ($z = 1.83$; Abdo et al. 2010), which underwent major flares in August–September 2008, reaching fluxes of the order of a few times 10^{-6} ph cm^{-2} s^{-1}. To further probe variability at short timescales we consider here the LAT light curves of two well studied FSRQs, 3C 454.3 ($z = 0.859$) and PKS 1510–089 ($z = 0.360$), for which the 1–day averaged flux above 100 MeV reached or even exceeded in few occasions 10^{-5} ph cm^{-2} s^{-1}. One of these events for PKS 1510–089 has been recently interpreted in the framework discussed above (Marscher et al. 2010). Such a large flux allows us to investigate variations occurring on timescales of the order of 3–6 hours, thus providing strong constraints on the theoretical scenarios.

2   LAT LIGHT CURVES

Light curves are derived by analysing the publicly available data with the standard Science Tools 9.15.2, including Galactic and isotropic backgrounds and the instrument response function P6 V3 DIFFUSE. For each time bin, we select the useful events and good-time intervals considering a zenith angle < 105 deg to avoid the Earth albedo and the photons within a region of interest with radius 10 degrees centred on the position of the source. Then we calculate the livetime, the exposure map and the diffuse response. Finally we analyse the data by using an unbinned likelihood algorithm (with the task `gtlike`) modelling the source spectrum with a power law

model, with integral flux (in the 0.1–100 GeV band) and photon index as free parameters. We plot in the light curves only the time intervals for which the corresponding test statistics (TS, Mattox at al. 1996; see also Abdo et al. 2009) is larger than 10, corresponding to a significance of roughly $\sqrt{TS} \simeq 3\sigma$. Due to the intense flux, with this condition only few bins are excluded from the light curves.

In Fig. 1 we report the light curves (in bins of 1 day) of PKS 1510–089 and 3C 454.3 covering about 1.5 years, from August 4 2008 (when regular LAT observations started) until January 31 2010. In both cases the light curves show extended periods of low flux level together with shorter period of intense activity.

2.1   Flux distributions and duty cycles

To characterise the variability we derive the distribution (differential and integral) of the fluxes of the daily light curve (Fig. 2). Basically these distributions can be used to characterise the γ–ray *duty cycle* of the blazars, usually defined as the fraction of time spent by the source in active states (e.g. Vercellone et al. 2004). We also take into account the (relatively large) errors on the fluxes reporting the average value in each bin with the corresponding standard deviation obtained performing Monte Carlo simulations of 1000 light curves varying the flux around the measured value with a gaussian distribution.

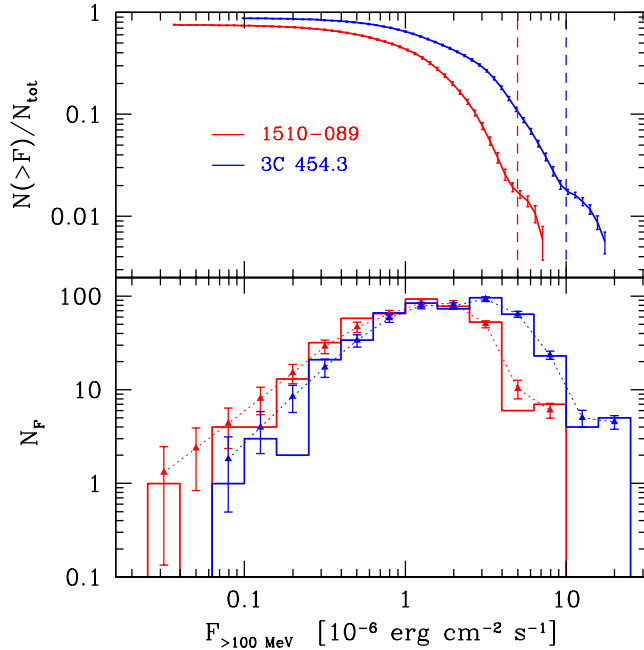Rather interestingly, for both sources the differential distribu-

Figure 2. *Upper panel*: The number of days (normalised to the total) for which the γ–ray flux above 100 MeV was above a given value F, as a function of the flux for both 1510–089 and 3C 454.3. Error bars report the uncertainties derived with Monte Carlo simulations (see text). Both sources displays a similar behaviour. The duration of the exceptional states studied in this work (vertical dashed lines) represents about 1% of the total life of the sources in the considered period. *Lower panel*: the solid histogram shows the flux distribution for both sources. Points (triangles) with the associated error bars are obtained by Monte Carlo simulations (text for details). Both sources display a peaked distribution, well described by an increasing power law $N_F \propto F^{1.5}$ up to the the peak and a fast decrease above it. The exceptional flares produce a tail at high fluxes (visible also as a bump in the integral distribution).

tion (lower panel) shows a well defined peak. Within the uncertainties, below the peak the distribution appears to be described by a power law with the same slope ($N_F \propto F^{1.5}$) in both sources. The peak defines the flux at which the sources spend most of the time. Low flux and high flux states are relatively less frequent, though it is more frequent for the source to be at lower fluxes than at higher ones.

Above the peak the distribution displays a rapid decrease, with, for both sources, a small excess of events at the highest fluxes (corresponding at about 10 times the mean flux), covering almost 1% of the total time, clearly related to the huge flares shown by the light curves. This can be considered the duty cycle of the sources for these extreme events for the epoch considered here.

Some *caveats* apply to our results: first of all both sources have been chosen because of the extreme activity they displayed in the considered past 1.5 years: as such, they cannot probably be considered as "typical" sources or in a typical state. A better characterisation of the flux distribution and duty cycle of the two sources would require to consider a more extended period of time, including also periods of lower activity. Indeed both sources during the EGRET observations (1991–2000) were at a lower flux level (see e.g. Nandikotkur et al. 2007, Hartman et al. 1999). If all flux states were considered, the duty cycle of the extreme events would be probably smaller than the 1% derived above.

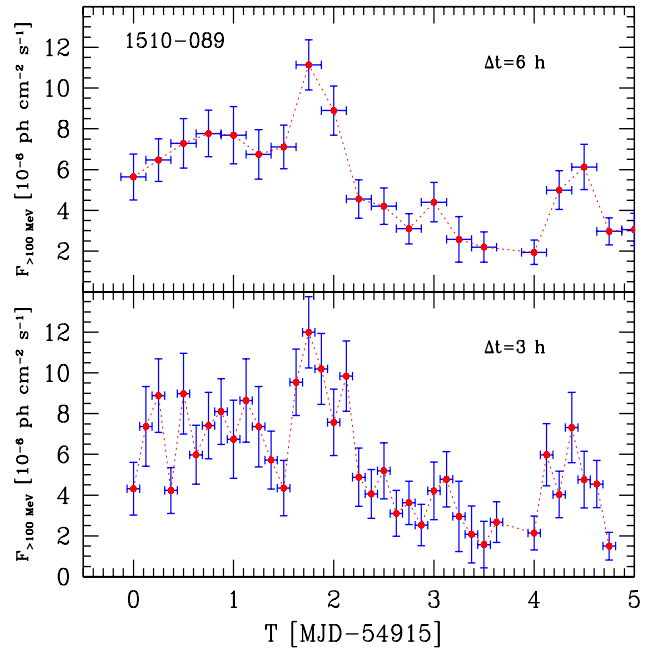A detailed discussion on the derived distributions is beyond

Figure 3. Light curve of PKS 1510–089 with bin–size of 6 hours (upper panel) and 3 hours (lower panel) starting on MJD 54915 (2009 March 25). Significant variations with timescales of 6 hours (and marginally also 3 hours) are clearly visible.

the scope of this paper. We only note that such a distribution, with a well defined power law from low to high fluxes and a rapid decrease at higher flux, is somewhat surprising, since log–normal distributions are currently discovered analysing X–ray light curves of both accretion powered sources (both galactic binaries and AGNs; e.g. Gaskell 2004, Uttley et al. 2005) and jetted AGNs (e.g. Giebels & Degrange 2009 for the case of BL Lac itself). A deeper discussion will be presented elsewhere.

2.2 Rapid variability

Looking at the daily light curve we selected periods of particular high flux (yellow vertical stripes in Fig.1), suitable to derive light curves in smaller time–bins. For PKS 1510–089 we choose two periods centred on MJD 54917 and MJD 54962, in which the source underwent strong outbursts ($F > 5 \times 10^{-6}$ ph cm^{-2} s^{-1} above 100 MeV) lasting 4–5 days. For 3C 454.3 we consider the recent period of exceptional γ–ray emission at the beginning of December 2009 (MJD 55160-55190). The maximum of the daily–averaged flux ($F \sim 2 \times 10^{-5}$ ph cm^{-2} s^{-1} above 100 MeV) was reached on December 2, 2009.

The resulting light curves, with binning of 6 hours (upper panels) and 3 hours (lower panels) are shown in Figs. 3, 4, (PKS 1510–089) and in Fig. 5 (3C 454.3). In both sources significant flux variations by a factor of 2 or more occurring on 6 hours timescale are clearly visible. Moreover, there are well defined events (MJD 54916.5 and 54917.2 for 1510–089, MJD 55167.5 for 3C 454.3) in which even at 3 hours there is evidence for variability (both in rising and decaying phases), although the relatively large errors prevent a secure conclusion.

Another feature of these light curve is the approximate symmetry of the peaks, (i.e. equal rising and decaying times) suggesting that the relevant timescale is the light crossing time of the emission
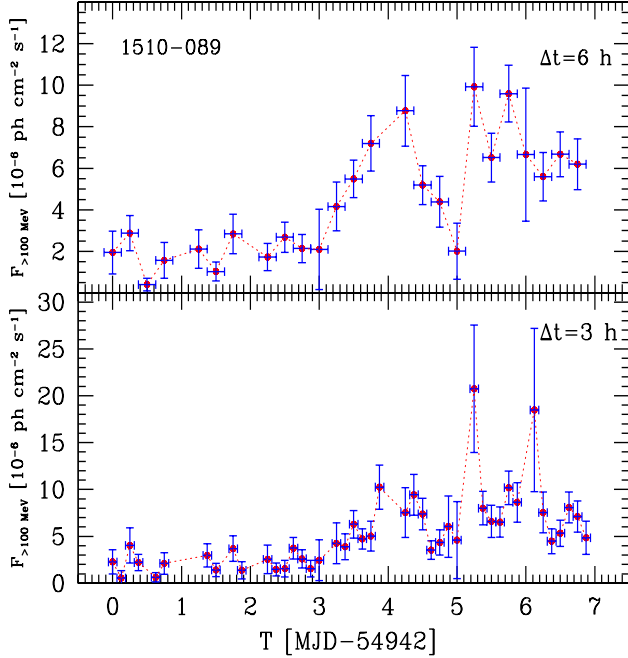
Figure 4. As Fig. 3, starting from MJD 54942 (2009 April 21).

Figure 5. As Fig. 3, for 3C 454.3 starting from MJD 55165 (2009 November 30).

region (e.g. Chiaberge & Ghisellini 1999). However, clearly, the statistics is not sufficient to make definite statements about the flare shapes. For example, the 1510-089 flare on MJD 54946 appears to have a distinctly longer rise than decay time scale.

3 DISCUSSION

The evidence of variability on hour time–scale is particular relevant for the modelling of the emission of the two blazars analysed here in periods of extreme activity. Specifically, the condition that the rise and the decay time is less than 6 (or even 3) hours puts robust constraints to the size (and consequently the location) of the γ–ray emitting region. Even considering the most conservative value of 6 hours we can constrain the (intrinsic) size of the emitting region to be $R < ct_{\rm var}\,\delta/(1+z) = 4.8 \times 10^{15}(\delta/10)$ cm and $3.5 \times 10^{15}(\delta/10)$ cm for PKS 1510–089 and 3C 454.3, respectively. Even considering extreme values of the Doppler factor, $\delta = 50$ we obtain values below 0.01 pc. This extremely small size is rather difficult to accommodate in the picture in which the emission takes place at very large distances ($\sim$10–20 pc) from the central black hole (e.g. Sikora et al. 2008, Marscher et al. 2010), unless the collimation angle of the jet is extremely small (Jorstad et al. 2005 derive an extremely small value, $\theta_{\rm jet} = 0.2$ deg, for both sources; however, using the same technique Pushkarev et al. 2009 found larger angles, 2–3 degrees). Putting a source with R given by our estimates at 20 pc yields $\theta_{\rm jet} \simeq 0.01\,(\delta/10)$ deg, much smaller than the value given by Jorstad et al. On the other hand, the constraint on the size from the variability can be more easily fulfilled if the emission region is located close to the black hole, as commonly assumed in the modeling of blazars (e.g. Tavecchio et al. 2000, Böttcher 2007, Kataoka et al. 2008, Ghisellini et al. 2010; see also Bonnoli et al. 2010). We conclude that the observation of short variability timescale disfavour the "far dissipation" scenario but can be accommodated in the more standard framework.
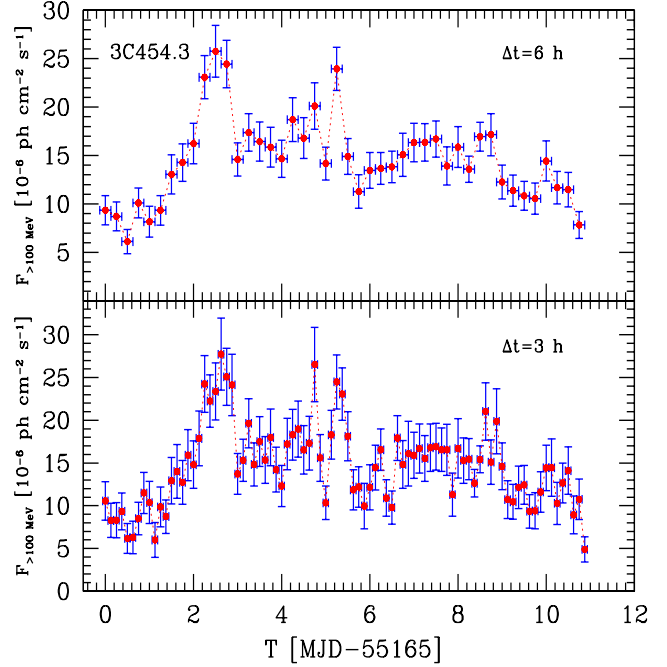
Another difference between the two models concerns the different cooling timescales of the emitting electrons, determined by the different value of the external radiation energy density. Specifically, the cooling time of electrons with Lorentz factor γ as measured in the observer frame is:

$$t_{\rm cool}^{\rm obs} = \frac{3m_e c\,(1+z)}{4\sigma_T\gamma\delta U'} \qquad (1)$$

where U' is the energy density (radiation plus magnetic) as measured in the jet frame. The Lorentz factor γ can be derived by the observed frequency $\nu_{\rm IC}$ of the IC photons: $\nu_{\rm IC} \approx \nu_{\rm ext}\gamma^2\,\Gamma\delta/(1+z)$, obtaining:

$$t_{\rm cool}^{\rm obs} = \frac{3m_e c}{4\sigma_T U'}\left(\frac{\nu_{\rm ext}}{\nu_{\rm IC}}\right)^{1/2}\left(\frac{\Gamma}{\delta}\right)^{1/2}(1+z)^{1/2} \qquad (2)$$

We assume as typical values for the physical quantities $\delta \sim \Gamma = 20$ and $\nu_{\rm IC} = 2.4 \times 10^{22}$ Hz (corresponding to an energy of 100 MeV). If the emission is produced by the inverse Compton scattering of external photons within the BLR we have $\nu_{\rm ext} = 2 \times 10^{15}$ Hz and $U' = 3.76 \times 10^{-2}\,\Gamma^2$ erg cm^{-3}. Instead, if the seed photons come from the torus we have $\nu_{\rm ext} = 3 \times 10^{13}$ Hz and $U' = 3 \times 10^{-4}\,\Gamma^2$ erg cm^{-3} (Ghisellini & Tavecchio 2008a). With these values we obtain observed cooling times of $t_{\rm cool} \simeq 800$ s (BLR) and $t_{\rm cool} \simeq 12,000$ s (torus). Both values are consistent with the observed timescale of variability. Therefore we cannot used the observed variability to distinguish between the two cases.

The same argument can be applied for variability in the X–ray band, in which the external IC emission is produced by electrons with much lower energy. Assuming $\nu_{\rm IC} = 1.2 \times 10^{18}$ Hz (i.e. 5 keV), Eq. 2 gives cooling times of the order of 31 hours in the case of the BLR scenario, and 20 days in the case of the torus. Clearly, observations of rapid variability in the X–ray band are difficult to explain in the "far dissipation" scenario. This discussion implicitly assumes that the observed X–rays come from the external IC mechanism; it is possible that in the X–ray band other emission mecha-

nism are effective: in particular the Synchrotron Self–Compton can contribute, especially in the soft X–ray band (i.e. ∼1 keV), where it can sometimes dominate the total flux.

Another interesting difference between the two scenarios, that can be exploited for further and possibly more conclusive tests, concerns the environment external to the region where γ–ray photons are produced and propagate. In fact, while in the standard view the γ–ray emission is expected to arise from the inverse Compton emission of soft photons of the BLR, at the distances considered in the "far dissipation" model the external radiation fields are dominated by the emission from the dusty torus. This difference directly translates in a different γ–ray spectral shape. If γ–rays are produced within the BLR the combined effects of the decrease of the scattering cross–section (Tavecchio & Ghisellini 2008) and of the possible absorption of γ–rays through pair conversion (e.g. Donea & Protheroe 2003, Liu, Bai & Ma 2008) would result in a spectral cut–off robustly predicted at energies of 10–20 GeV (e.g. Ghisellini & Tavecchio 2009). In the case of the "far dissipation" scenario, instead, these effects would imprint a cut–off at much larger energies (∼ 1 TeV). Therefore, the observation of a spectrum extending up to few tens of GeV would rule out the standard one–zone model located within the BLR.

One cannot exclude, however, that more than one component, located at different regions from the central black hole, are simultaneously active. In this view it is conceivable that inner regions, emitting within the BLR, produces the bulk of the fast varying GeV component, while more external regions, beyond the BLR can contribute to the emission above 100 GeV. This could explain the detection of emission above 100 GeV in 3C 279 (Albert et al. 2008) and in 1510–089 (Wagner 2010[1]). If this is would be the case, the overall SED would be complex, with different frequency bands dominated by regions at different locations (e.g. Ghisellini & Tavecchio 2009). Also the variability would be complex, with the possibility to have a rapidly varying GeV emission accompanied by a TeV emission varying on much longer timescales. We finally note that in the current view of FSRQs, the detection of a rapidly varying (∼ hours) TeV emission would be quite difficult to explain, since it would require to be produced at large distances (to avoid the absorption of photons by the optical–UV radiation of the BLR) but in a region not larger than $\sim 10^{16}$ cm. Similarly to the case of the ultrafast variability observed in PKS 2155–304 (Aharonian et al. 2007), this would require to assume the presence of "needles" of emission within the more extended jet (e.g. Ghisellini & Tavecchio 2008b, Giannios et al. 2009).

4 CONCLUSION

We have analysed the LAT light curves of the two FSRQs 3C 454.3 and 1510–089 from August 2008 to January 2010. In this period the two sources displayed several γ–ray flares with fluxes approaching or even exceeding 10^{-5} ph cm^{-2} s^{-1}.

We have characterised the variability of the two sources deriving the distribution of the fluxes. We found that in both cases this distribution is well approximated by an increasing power low at low fluxes ($N_F \propto F^{1.5}$) up to a peak above which the probability rapidly decreases. These cases are therefore different from those well described by log–normal distributions recently found in both accreting systems and blazars in the X–ray band.

We have derived light curves around the epochs of the largest flares with bins of 3 and 6 hours, finding that there are several cases in which the flux varies on these timescales, with variations even larger than a factor of 2. This implies a correspondingly very compact emitting region that is difficult to be explained by models that assume that most of the γ-ray emission is produced in regions far away from the central engine, at distances of tens of parsecs. The same conclusion, i.e. that the bulk of the emission is produced close to the central engine, was also independently reached by Kovalev at al. (2009), using a different approach.

REFERENCES

Abdo A. A., et al., 2010, ApJ, 710, 810
Abdo A. A., et al., 2009, ApJ, 697, 934
Aharonian F., et al., 2007, ApJ, 664, L71
Atwood W. B., et al., 2009, ApJ, 697, 1071
Böttcher M., 2007, Ap&SS, 309, 95
Bonnoli G., Ghisellini G., Foschini L., Tavecchio F., Ghirlanda G., 2010, MNRAS, submitted (arXiv:1003.3476)
Chiaberge M., Ghisellini G., 1999, MNRAS, 306, 551
Donea A.-C., Protheroe R. J., 2003, APh, 18, 377
Gaskell C. M., 2004, ApJ, 612, L21
Ghisellini G., Tavecchio F., 2008a, MNRAS, 387, 1669
Ghisellini G., Tavecchio F., 2008b, MNRAS, 386, L28
Ghisellini G., Tavecchio F., 2009, MNRAS, 397, 985
Ghisellini G., Tavecchio F., Foschini L., Ghirlanda G., Maraschi L., Celotti A., 2010, MNRAS, 402, 497
Giannios D., Uzdensky D. A., Begelman M. C., 2009, MNRAS, 395, L29
Giebels B., Degrange B., 2009, A&A, 503, 797
Jorstad S. G., et al., 2005, AJ, 130, 1418
Hartman R. C., et al., 1999, ApJS, 123, 79
Kataoka J., et al., 2008, ApJ, 672, 787
Kovalev Y. Y., et al., 2009, ApJ, 696, L17
Larionov V. M., et al., 2008, A&A, 492, 389
Liu H. T., Bai J. M., Ma L., 2008, ApJ, 688, 148
Marscher A. P., et al., 2008, Natur, 452, 966
Marscher A. P., et al., 2010, ApJ, 710, L126
Mattox J. R., et al., 1996, ApJ, 461, 396
Nandikotkur G., Jahoda K. M., Hartman R. C., Mukherjee R., Sreekumar P., Böttcher M., Sambruna R. M., Swank J. H., 2007, ApJ, 657, 706
Pushkarev A. B., Kovalev Y. Y., Lister M. L., Savolainen T., 2009, A&A, 507, L33
Sikora M., Moderski R., Madejski G. M., 2008, ApJ, 675, 71
Sikora M., Stawarz Ł., Moderski R., Nalewajko K., Madejski G. M., 2009, ApJ, 704, 38
Sokolov A., Marscher A. P., McHardy I. M., 2004, ApJ, 613, 725
Tavecchio F., et al., 2000, ApJ, 543, 535
Tavecchio F., Ghisellini G., 2008, MNRAS, 386, 945
Uttley P., McHardy I. M., Vaughan S., 2005, MNRAS, 359, 345
Vercellone S., Soldi S., Chen A. W., Tavani M., 2004, MNRAS, 353, 890

---

[1] HEAD meeting 2010, https://www.confcon.com/head_2010/